Plant Biotechnology 31, 159–165 (2014)
DOI: 10.5511/plantbiotechnology.14.0222a

Original Paper

Arabidopsis glycerol-3-phosphate permease 4 is localized in the plastids and involved in the accumulation of seed oil

Hiromitsu Kawai[1], Toshiki Ishikawa[1], Toshiaki Mitsui[2], Shin Kore-eda[3], Maki Yamada-Kawai[1], Jun-ichi Ohnishi[1,*]

[1] Graduate School of Science and Engineering, Saitama University, Saitama 338-8570, Japan; [2] Graduate School of Science and Technology, Niigata University, Niigata 950-2181, Japan; [3] Comprehensive Analysis Center for Science, Saitama University, Saitama 338-8570, Japan
* E-mail: ohnishi@molbiol.saitama-u.ac.jp Tel: +81-48-858-3397 Fax: +81-48-858-3384

Received February 4, 2014; accepted February 22, 2014 (Edited by M. Yamaguchi)

Abstract In plant cells, glycerol 3-phosphate (G3P) is apparently able to permeate the plastid envelope, but no specific transporter has been characterized so far. The *Arabidopsis* five G3Pp proteins have been predicted as putative G3P permeases because of their high homologies with the prokaryotic G3P/phosphate antiporter GlpT. In the present study, G3Pp4 was characterized in detail utilizing reverse genetic approaches. Promoter analysis using GUS expression revealed that *G3Pp4* was expressed strongly throughout the embryos during late developmental stages, and the seed lipid contents decreased in two *g3pp4* knockout mutants. An enhanced yellow fluorescent protein-fused G3Pp4 was localized in the plastids, functioned physiologically in *A. thaliana*, and had G3P-transport activity in *E. coli*. These results suggest that *Arabidopsis* G3Pp4 is a plastid envelope-localized G3P transporter and involved in accumulation of storage lipids in late embryogenesis.

Key words: Arabidopsis, glycerol 3-phosphate, plastid, transporter, triacylglycerol.

In plant cells, fatty acids are synthesized de novo only in the plastids, whereas glycerolipid biosynthesis takes place in two subcellular compartments: in the "prokaryotic" pathway within the plastids and the "eukaryotic" pathway outside of the plastids (Ohlrogge and Browse 1995). Glycerol 3-phosphate (G3P) is an obligate precursor in the initial step of glycerolipid synthesis, and also a factor influencing the balance of the above two glycerolipid synthesis pathways (Gardiner et al. 1982; McKee and Hawke 1979; Roughan et al. 1980). In *A. thaliana*, G3P is synthesized either from glycerol catalyzed by the glycerol kinases in the cytosol (Eastmond 2004; Lu et al. 2001), or from the glycolysis/photosynthesis intermediate dihydroxyacetone phosphate (DHAP) catalyzed by the DHAP reductases (DHAPRs) both in the cytosol and the plastids (Chanda et al. 2011).

Recent studies about the plant immune response suggest that a significant amount of G3P is transported between the cytosol and the plastids. Systemic acquired resistance (SAR), a plant disease-resistance mechanism, utilizes G3P as a signaling molecule that can move throughout the plant and induce the activation of broad-spectrum resistance reactions (Chanda et al. 2011). During the initial SAR response, G3P is accumulated, resulting in up-regulation the expression of DIR1 and AZI1, the factors essential for SAR in *A. thaliana* (Yu et al. 2013). Interestingly, the expression of both is greatly reduced and the SAR response is almost negated by the disruption of *SFD1*, a plastid-localized DHAPR-coding gene. Furthermore, this *sfd1* mutant phenotype was restored by application of exogenous G3P (Chanda et al. 2011; Yu et al. 2013). These results suggest the existence of G3P transporters in the plastid envelope and in the plasma membrane.

Studies of prokaryotic lipid synthesis and plastid phosphate translocator also suggest that G3P is transported across the plastid inner membrane (Chanda et al. 2011; Kunst et al. 1988; Shen et al. 2010; Sparace and Mudd 1985; Weber et al. 2005; Xue et al. 1997; Yu et al. 2013). In isolated chloroplasts from spinach leaves, the uptake activity of inorganic phosphate (Pi) is due to the triose phosphate translocator (TPT) principally, and inhibited by application of G3P partially (Fliege et al. 1978). TPT belongs to the drug/metabolite transporter superfamily, but these transporter have very low affinity for G3P (Linka et al. 2008). These results suggest existence of unknown transporters for uptake of Pi that compete with G3P in the plastid envelope.

Abbreviations: CDS, coding DNA sequence; CLSM, confocal laser microscopy; DAF, days after flowering; DHAP, dihydroxyacetone phosphate; EYFP, enhanced yellow fluorescence protein; G3P, glycerol 3-phosphate; G3Pp, glycerol-3-phosphate permease; GUS, β-glucuronidase; MFS, Major Facilitator Superfamily; SAR, systemic acquired resistance; T-DNA, transfer DNA; TG, triacylglycerol.

This article can be found at http://www.jspcmb.jp/
Published online May 2, 2014

In bacterial species, G3P transporters have been identified and characterized (Castañeda-García et al. 2009; Law et al. 2007; Song et al. 1998). GlpT, a member of the major facilitator superfamily (MFS), is a G3P transporter that exchanges Pi and G3P in *E. coli* (Law et al. 2007). In *A. thaliana*, five proteins have been identified as GlpT homologues and classified as members of the G3P permease (G3Pp) family, which is involved in phosphate homeostasis (Ramaiah et al. 2011). However, none of these have yet been characterized as to transport activity and subcellular localization.

Herein, we report that G3Pp4, a member of the *Arabidopsis* G3Pp family, exhibits G3P transport activity. Furthermore, the data presented here strongly suggest that G3Pp4 protein is localized in the plastids and involved in the accumulation of storage lipid during late embryo development.

Materials and methods

Plant materials and growth conditions

Wild-type *A. thaliana* (ecotype Columbia-0) was obtained from the Arabidopsis Biological Resource Center (ABRC) at Ohio State University (Alonso et al. 2003). The seeds were surface-sterilized in a solution containing 0.3% (v:v) sodium hypochlorite and 0.5×10^{-3}% (v:v) Tween® 20. Surface-sterilized seeds were then sown on soil in pots. For observation of hypocotyls and roots, seeds were sown on 0.9% (w:v) agar medium containing half-strength Murashige and Skoog (MS) salts (Murashige and Skoog 1962), Gamborg B5 vitamins (Gamborg et al. 1968), 1% (w:v) sucrose, and 0.05% (w:v) MES-KOH (pH 5.7). Both pots and plates were incubated at 2°C in darkness to break seed dormancy, then were transferred into the Biotron growth chamber (LPH220S, Nippon Medical & Chemical Instruments, Osaka, Japan) under a light/dark cycle of 14 h/10 h, day/night temperatures of 23°C/18°C, and 60% relative humidity.

DNA extraction

For cloning and genotyping, DNA was extracted from rosette leaves of each line. Leaf samples were homogenized in an extraction buffer containing 0.2 M Tris-HCl (pH 9.0), 0.4 M LiCl, 25 mM EDTA, and 1% (w:v) SDS. Homogenates were then extracted with an equal volume of phenol : chloroform : isoamyl alcohol (25 : 24 : 1, v : v : v), followed by chloroform extraction. DNA in the aqueous phase was precipitated by adding an equal volume of isopropyl alcohol.

Isolation of G3Pp4 disruptants

Two T-DNA-tagged knockout mutant alleles for *G3Pp4* (At4g17550), SALK_071338C (*g3pp4-1*; Alonso et al. 2003; Ramaiah et al. 2011) and GK-230D07, were obtained from the ABRC and the GABI-Kat (Kleinboelting et al. 2012), respectively. Each mutant was selected by antibiotic resistance and PCR-based genotyping. The pairs of gene-specific primers used for the screening of insertions into the *G3Pp4* gene included SalI-AtG3Pp4atg (5′-ttggtcgacatggcgatgaattcgaaga-3′) and salkLBb1 (5′-gcgtggaccgcttgctgcaact-3′) for *g3pp4-1*, or AtG3Pp4opal-KpnI (5′-ctggtacctcatcttctatcggttaacag-3′) and o8409 (5′-atattgaccatcatactcattgc-3′) for GK-230D07. The homozygous line obtained from GK-230D07 was named *g3pp4-2*.

Reverse transcription reaction and PCR

For reverse transcription reactions, RNA samples were extracted from each tissue of *Arabidopsis* using an RNeasy Plant Mini Kit (QIAGEN, Venlo, Netherlands) according to the manufacturer's instructions. Each RNA sample was used as a template for cDNA synthesis using PrimeScript cDNA Synthesis Kit (Takara, Otsu, Japan) and each cDNA sample was then used for cloning and semi-quantitative RT-PCR using Phusion® HF DNA Polymerase (New England Biolabs, Ipswich, MA) according to the manufacturer's instructions. The gene-specific primer pairs used for the RT-PCR included SalI-AtG3Pp4atg and AtG3Pp4opal-KpnI for the full-length *G3Pp4* coding DNA sequence (CDS), and eif4A1F (5′-ccagaaggcacacagtttgatgca-3′) and eif4A1R (5′-tcatcatcacgggtcacgaaattg-3′) for *eIF4A1* as a control.

Extraction and analysis of lipids

Dry seeds of *Arabidopsis* (10 mg) were immersed in 1 ml of boiling 2-propanol for several minutes and then chilled on ice. Lipids were then extracted according to Folch et al. (1957). Total lipid extracts (1 mg) were separated into respective lipid classes by thin layer chromatography using 20×20 cm TLC Silica gel 60 glass plates (Merck Millipore, Darmstadt, Germany). Hexane : diethyl ether : acetate (8 : 3 : 1, v : v : v) was used as a development solvent to separate lipids in the samples. Lipid spots were visualized by spraying plates with primuline (0.01% (w:v) in 80% (v:v) acetone) and illuminating them with ultraviolet light, and then scraped off. Triacylglycerol-class lipids were subjected to methanolysis at 80°C for 3 h in 3 ml of 5% (w:v) HCl in methanol, with an additional 47.8 nmol pentadecanoic acid as an internal standard and 50 nmol 2,6-di-*t*-butyl-4-methylphenol as an antioxidant. The resultant fatty acid methyl esters were extracted with 3 ml of hexane. Lipid content was determined by quantifying fatty acid methyl esters with a gas chromatograph-mass spectrometer (GCMS-QP2010, Shimadzu, Kyoto, Japan) equipped with a TC-70 capillary column (0.25 mm ϕ, 60 m, GL Science, Tokyo, Japan) under temperature programming (increasing from 120 to 240°C at 6°C min^{-1}). The temperature for the injector chamber was set at 250°C. Helium was used as the carrier gas at a flow rate of 4.3 ml min^{-1}, under ionization voltage of 70 eV.

Construction of expression vectors

To generate the Ti plasmid expressing *uidA* under the control of the *G3Pp4* promoter, a fragment containing an upstream region of *G3Pp4* and part of the CDS of *G3Pp4* (Pro_{G3Pp4}) was amplified by PCR using the Phusion® HF

DNA Polymerase and the primer set of, G3Pp4m1875F (5′-cgattaggagaatcaacacatacc-3′) and G3Pp4p60R (5′-ctgactctcctcagaagcgc-3′). This amplified fragment was then cloned into the pT7Blue T-vector (Merck Millipore, Darmstadt, Germany), and excised as a SbfI-BamHI fragment. This fragment was subcloned into pBI121 (Clontech, Mountain View, CA) in place of the $Pro_{CaMV35S}$ region (pBI121-$Pro_{CaMV35S}$::*GUS*). To generate Ti plasmid for the expression of the *EYFP-G3Pp4* fusion protein, the CDS of *G3Pp4* was amplified by PCR using the cDNA as a template and the primers SalI-G3Pp4atg and G3Pp4opal-KpnI. The CDS of *G3Pp4* was subsequently cloned into the entry vector pENTR11-E, a derivative of the pENTR11 dual selection vector (Life Technologies, Carlsbad, CA) with the deletion of *ccdB* and *cat* genes, then subcloned into pGWB542 (Tanaka et al. 2011) using the LR reaction with LR Clonase™ Enzyme Mix (Life Technologies, Carlsbad, CA) according to the manufacturer's instructions to create the expression clone (pGWB542-*EYFP-G3Pp4*). These expression clones were then transformed into *Agrobacterium tumefaciens*.

Transformation of plant materials

Arabidopsis transformants were produced using the floral dip method (Clough and Bent, 1998) with *A. tumefaciens* EHA105 containing the above Ti plasmids. Transgenic lines with a single T-DNA insertion were selected by antibiotic resistance and PCR-based genotyping, as described above.

For transient expression, epidermal peels of onion (*Allium cepa*) bulbs were placed onto MS agar medium. The peels were bombarded with 1.8 μm tungsten particles (Japan New Metals, Toyonaka, Japan) coated with pGWB542-*EYFP-G3Pp4* and p*WxTP-DsRed* (Kitajima et al. 2009) using the particle delivery system (PDS-1000/He, Bio-Rad, Hercules, CA) with a bombardment pressure of 1100 p.s.i. under vacuum. The tissues were incubated for 16 h at 23°C in the dark, then were observed with a confocal laser scanning microscope (CLSM; Eclipse TE-2000, Nikon, Tokyo, Japan).

Histochemical staining of β-glucuronidase (GUS) activity

For histochemical staining of GUS activity, tissues of transgenic *Arabidopsis* expressing Pro_{G3Pp4}::*uidA* gene were fixed with 90% (v:v) acetone at -20°C for 1 h, and then washed twice with 100 mM sodium phosphate buffer (pH 7.4).

To detect GUS activity, each tissue was incubated in a staining solution containing 0.5 mM 5-bromo-4-chloro-3-indolyl-β-D-glucuronide, 0.5 mM potassium ferricyanide, and 50 mM sodium phosphate buffer (pH 7.4) at room temperature overnight in darkness, then washed and dehydrated with an ethanol : water series (1 : 9, 3 : 7, 5 : 5, 7 : 3, v:v) at room temperature. These stained tissues were rehydrated through the ethanol : water series in reverse order, then were incubated in a preservation solution containing 25% (v:v) glycerol and 5% (v:v) ethanol prior to the observation under a stereomicroscope (SMZ-1500, Nikon, Tokyo, Japan) or a phase-contrast microscope (Eclipse TE-2000, Nikon, Tokyo, Japan). For staining the embryo samples, both valves of the siliques were incised prior to fixation. After rehydration, the embryos were exposed for the microscopy.

G3P transport activity measurement using the whole cell assay

E. coli strain JW2234 was obtained from the National BioResource Project (NBRP) and used as the *ΔglpT* strain, a *glpT* disruptant (Baba et al. 2006). The G3P uptake activity of *ΔglpT* strains transduced with the expression vector or a control vector was measured according to the whole cell assay (Law et al. 2007).

Results

G3Pp4 is strongly expressed in embryos

To identify the tissue-specificity of *G3Pp4* expression, a fragment including 1875 bp upstream from the start codon plus the initial 60 bp of the CDS was used as a promoter for the expression of GUS reporter gene (Pro_{G3Pp4}-*GUS*) on the Ti plasmid, pBI121 (Jefferson et al. 1987). This Pro_{G3Pp4}-*GUS* plasmid was introduced into *A. tumefaciens* and used to transform *Arabidopsis*

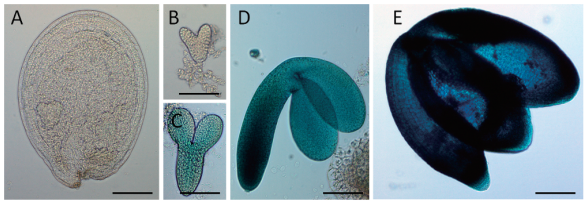

Figure 1. Analysis of *G3Pp4* expression during *Arabidopsis* embryogenesis by Pro_{G3Pp4}::*GUS*. (A–E) GUS-staining in the embryo during early heart stage (A), late heart stage (B), linear cotyledon stage (C), bending cotyledon stage (D) and mature green stage (E). Scale bars, 100 μm.

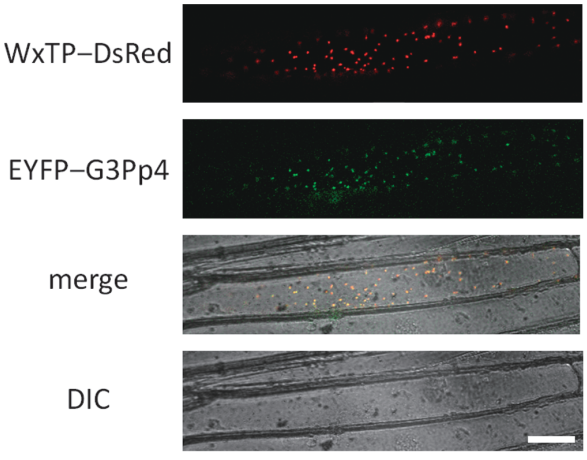

Figure 2. Subcellular localization of G3Pp4. The *EYFP-G3Pp4* fusion gene under the control of the CaMV35S promoter was co-expressed with *WxTP-DsRed* transiently in onion epidermal cells. Scale bar, 50 μm.

ecotype Columbia-0. Histochemical staining of transgenic *Arabidopsis* expressing Pro_{G3Pp4}-*GUS* indicated that *G3Pp4* was expressed in roots, the vascular system, stomatal guard cells, anthers, pollen grains (Supplemental Figure S1), and embryos, especially during the later development stages (Figure 1). These results are in agreement with the AtGenExpress microarray data (Schmid et al. 2005).

EYFP-G3Pp4 fusion protein is localized to plastids

To investigate the subcellular localization of G3Pp4, an enhanced yellow fluorescent protein (EYFP) was fused to G3Pp4 and expressed transiently in onion epidermis cells under control of the *Cauliflower mosaic virus 35S* promoter ($Pro_{CaMV35S}$). By CLSM, the fluorescence signal of EYFP-fused G3Pp4 (EYFP-G3Pp4) was co-localized with that of DsRed fused with a plastid transit peptide (Kitajima et al. 2009), indicating that G3Pp4 is localized in plastids, and probably is an envelope transporter (Figure 2).

g3pp4 mutations decrease the amount of seed storage lipid

To characterize the physiological roles of G3Pp4, two independent T-DNA insertion lines, *g3pp4-1* (Alonso et al. 2003; Ramaiah et al. 2011) and *g3pp4-2* (Kleinboelting et al. 2012), were obtained. As shown in Figure 3A, each line has a T-DNA insertion in the first exon. When the transcript levels of *G3Pp4* were checked by RT-PCR, no amplification products were detected in *g3pp4-1* and *g3pp4-2* plants (Figure 3B).

Homozygous *g3pp4-1* and *g3pp4-2* mutant plants were morphologically identical throughout development and reached similar size to that of wild-type plants. Also, the fertility of *g3pp4* mutants was the same as wild-type plants. No difference was found in pollen grain size and shape between the wild type and *g3pp4* when observed under SEM (data not shown).

Because *G3Pp4* encodes a putative glycerol-3-phosphate permease and is expressed strongly in the developing embryo, we analyzed the storage substances in the seeds and evaluated whether *g3pp4* mutation affected biochemical processes during the embryogenesis (Table 1). Compared with wild type, dry weight of total lipids of mutant seeds were reduced, although no differences in the average weight of the seeds were found in the mutants. Furthermore, triacylglycerol (TG) contents per seed lipid of both mutants were also lower than that of wild type. From these data, TG contents per seed dry weight of both mutants were decreased to 68% of the wild type (Table 1). In addition, the fatty acid compositions of TG in wild type and *g3pp4* seeds were analyzed (Table 2). The total proportion of very long chain fatty acids in TG was slightly decreased in *g3pp4* mutant.

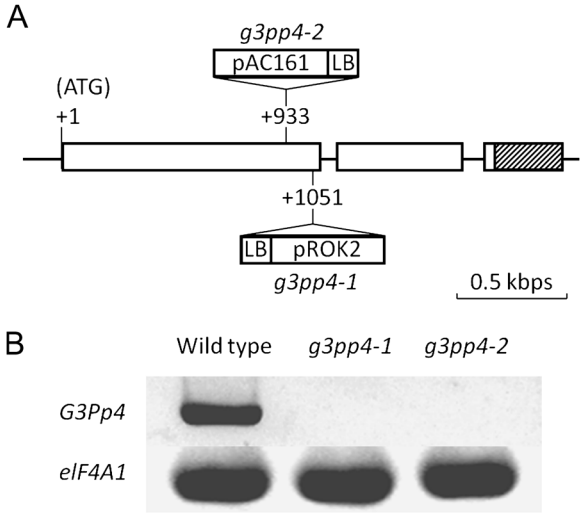

Figure 3. Structure of the *G3Pp4* gene carrying a T-DNA insertion, and the expression of *G3Pp4* in *g3pp4* mutant lines assayed by RT-PCR. (A) Exon/intron structure of the *G3Pp4* gene showing the locations (relative to the start codon) of insertion sites identified in T-DNA mutants. Open boxes represent exons and shaded boxes represent 3'UTR. LB, left border of the T-DNAs for which the precise integration sites could be identified; pROK2, T-DNA present in the Salk collection; pAC161, T-DNA present in the GABI-KAT collection. (B) RT-PCR analysis of the *G3Pp4* transcript in wild-type and mutant (*g3pp4-1* and *g3pp4-2*) rosette leaves. Approximately 0.1 μg of total RNA was used in each PCR, and *eIF4A1* (At3g13920) was used as a control.

Table 1. Lipid analysis of wild-type and *g3pp4* dry seeds.

	Dry weight per seed (μg)	Lipid content per seed (μg)	TG amounts per seed (nmol)
Wild type	24.85±0.76	10.88±0.53	11.86±0.11
g3pp4-1	25.65±0.50	8.71±1.50	8.12±1.90
g3pp4-2	25.25±0.52	8.99±0.37	7.91±0.34

Each value is an average of three independent measurements.

Table 2. Fatty acid composition of TG purified from wild-type and *g3pp4* seeds.

	Fatty acid composition (mol %)		
	Wild type	*g3pp4-1*	*g3pp4-2*
Long chain fatty acids			
C16:0	7.53±0.28	7.86±0.06	8.06±0.28
C16:1	n.d.	n.d.	n.d.
C16:2	n.d.	n.d.	n.d.
C16:3	n.d.	n.d.	n.d.
C18:0	4.18±0.32	4.04±0.38	4.00±0.35
C18:1	15.64±0.14	17.00±0.62	16.31±0.59
C18:2	25.86±0.60	26.78±1.28	26.92±1.02
C18:3	13.50±0.62	14.28±0.63	14.82±0.38
Very long chain fatty acids			
C20:0	2.97±0.15	2.83±0.26	2.87±0.20
C20:1	27.38±0.67	24.59±1.40	24.38±0.76
C22:0	0.35±0.04	0.32±0.03	0.34±0.06
C22:1	0.34±0.02	0.33±0.06	0.34±0.05
C24:0	2.31±0.05	1.98±0.28	1.96±0.14

n.d. indicates not detected.

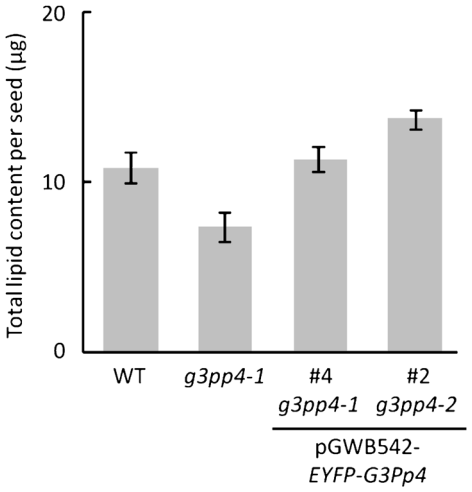

Figure 4. Complementation test of *g3pp4* mutant phenotype with overexpression of EYFP-G3Pp4. Total lipid contents per seed of wild-type (WT) Columbia-0 *Arabidopsis*, nontransformed *g3pp4-1* mutant, and *g3pp4* mutants transformed with the pGWB542-*EYFP-G3Pp4* vector. Each value is an average of three independent expreriments.

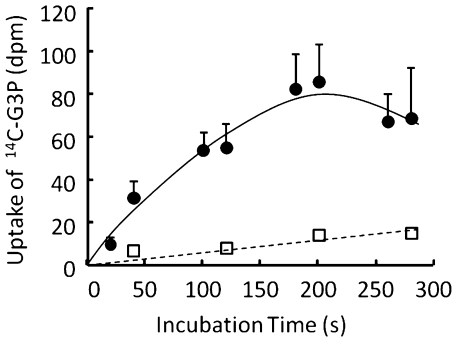

Figure 5. Functional analysis of EYFP-G3Pp4. G3P uptake of *E. coli* *ΔglpT* strains transformed with the pGWB542-*EYFP-G3Pp4* vector (●, the solid line) or the empty vector (pGWB542-*EYFP*; □, the broken line). Each value is an average of three independent expreriments.

To determine whether the defects in the mutant seeds were caused by *G3Pp4* disruptions, we generated transgenic plants expressing EYFP-fused G3Pp4 (EYFP-G3Pp4) driven by $Pro_{CaMV35S}$ in the *g3pp4* mutants. As shown in Figure 4, overexpression of *EYFP-G3Pp4* complemented the total lipid contents in the seed of the *g3pp4* mutants. These results indicate that the knockout of *G3Pp4* affected the seed storage lipid contents, which are synthesized during late embryogenesis (Goldberg et al. 1994) when *G3Pp4* is strongly expressed (Figure 1).

Additionally, we confirmed the subcellular localization of G3Pp4 using *g3pp4* mutants expressing EYFP-G3Pp4. By using CLSM, EYFP signal was detected only in the chloroplasts (Supplemental Figure S2), consistent with the result of transient expression (Figure 2).

G3Pp4 has a G3P transporter activity in E. coli

To investigate whether G3Pp4 protein could perform G3P transport, *EYFP-G3Pp4* was expressed under the control of $Pro_{CaMV35S}$ by transducing pGWB542-*EYFP-G3Pp4* into the *E. coli ΔglpT* strain. In the whole-cell uptake assay, significant radioactivity from ^{14}C-G3P was detected in *ΔglpT* strains transfected with the *EYFP-G3Pp4* plasmid, but not in *ΔglpT* transfected with a control vector (Figure 5). This result suggests that G3Pp4 actually functions as a G3P transporter.

Discussion

In *A. thaliana*, five members of the G3Pp family had been identified as homologues of the *E. coli* G3P transporter GlpT (Ramaiah et al. 2011), although none of these had so far been characterized for transporter activities and subcellular localizations. Initially, we attempted the TA cloning method and also the directional cloning method using inducible expression vectors such as pET and pBAD to clone *G3Pp4*, but without success. We concluded that our initial efforts to clone the *G3Pp* genes might have been hindered by the toxicity of these proteins in *E. coli* cells, because some members of the MFS are reportedly difficult to be cloned or expressed in homologous and heterologous systems due to their toxicity (Elashvili et al. 1998; Frohlich et al. 2010; Gubellini et al. 2011). In the present study, fortunately, *G3Pp4* was successfully cloned into an entry vector for the Gateway™ Cloning System. Subsequent sub-cloning with the LR reaction allowed expression of EYFP-G3Pp4 driven by $Pro_{CaMV35S}$, a promoter with very weak activity in *E. coli* (Assaad and Signer, 1990; Lewin et al. 2005), which might have mitigated the toxicity of G3Pp4. Finally, we were able to show that the uptake of G3P was enhanced significantly in the *E. coli ΔglpT* strain transformed with pGWB542-*EYFP-G3Pp4* (Figure 5).

The promoter-GUS assay revealed that *G3Pp4* was expressed in late stages of embryogenesis (Figure 1), but not in the source tissues (Supplemental Figures S1A, B, C). This suggests that the observed decrease in seed storage lipid in the *g3pp4* mutants might be due not to carbon-translocation from source tissues, but to a change in the metabolism of the embryo itself (Table 1). Our results indicating *G3Pp4* expression during late embryogenesis is consistent with previously published microarray data (Craigon et al. 2004), but not with the results of another report that also utilized promoter-GUS analysis (Ramaiah et al. 2011). Because the length of the promoter region which we used is longer than that in the previous reports, the extended region might contribute to the significant expression in embryos (Figure 1).

The decrease of seed lipid detected in two independent *g3pp4* mutants (Table 1) and its restoration by the overexpression of *EYFP-G3Pp4* (Figure 4) indicates that this phenotype is attributed to the disruption of *G3Pp4*. Furthermore, EYFP-G3Pp4 localized in the plastids (Figure 2 and Supplemental Figure S2). All these

results indicate that G3Pp4 is a plastid-localized G3P transporter, expressed during late embryogenesis and supply G3P to the cytosol to be used for storage lipid synthesis in the endoplasmic reticulum (ER) (Bates et al. 2013).

In *A. thaliana*, the rate-limiting enzyme for storage lipid synthesis is thought to be GPAT9, which is oriented in the ER membrane with its active site facing the cytosol (Gidda et al. 2009). When glycerolipid synthesis in the ER is strongly activated, significant amounts of G3P need to be synchronously supplied in the cytosol. However, it has been known that several cytosolic enzymes involved in G3P biosynthesis are inhibited by the accumulation of G3P itself, such as phosphoglucose isomerase and DHAPR (Kito and Pizer 1969; Klöck and Kreuzberg 1989; Quettier et al. 2008). Therefore eukaryotic glycerolipid synthesis might require G3P supply independent of the cytosolic biosynthetic pathway. In plant cells, G3P is synthesized also in the plastids (Chanda et al. 2011). When the supply of G3P from the plastids is critical for the eukaryotic glycerolipid synthesis, the disruption of plastidic G3P transporter will affect eukaryotic lipid synthesis. In fact, lipid content was reduced in *g3pp4* seeds (Table 1) which lack a plastid-localized G3P transporter in the embryos (Figures 1 and 2).

As detailed above, G3P is transported across the plastid envelope (Chanda et al. 2011; Kunst et al. 1988; Sparace and Mudd 1985; Shen et al. 2010; Xue et al. 1997; Yu et al. 2013). However, there is almost no expression of *G3Pp4* in the major photosynthetic tissues of *Arabidopsis* leaves (Supplemental Figure S1), suggesting that some other members of the G3Pp family might be involved in the chloroplastic transport of G3P in the leaves. Furthermore, disruption of *G3Pp4* has been observed to affect only seed lipid contents so far (Table 1), although *G3Pp4* expression is detected in other tissues (Supplemental Figure S1). This result suggests that other members of the G3Pp family might compensate for the loss of G3Pp4 function in tissues other than in the embryo. Among the family members, G3Pp5, which has a predicted N-terminal plastid transit peptide (Emanuelsson et al. 1999; Petsalaki et al. 2006) and is expressed in mature pollen and stomatal guard cells (Craigon et al. 2004; Ramaiah et al. 2011) overlapping with *G3Pp4* expression, might function redundantly with G3Pp4. Additionally, investigation of SAR suggested the mobility of G3P across the plasma membrane (Chanda et al. 2011) and its trafficking throughout the plant via phloem. This suggests that plasma membrane has the G3P export pathway in infected cells and the G3P import pathway in distal non-infected cells. Other members of G3Pp family might be involved in the transport of G3P across the plasma membrane.

The continued investigation of the *Arabidopsis* G3Pp family should provide new insights into the dynamic metabolite exchange that occurs between plastids and the cytoplasm, and also across the plasma membrane.

Acknowledgements

We thank Prof. T. Kotake for kindly supplying the pBI121 vector; Prof. T. Nakagawa for supplying the pGWB destination vectors; the Salk Institute Genomic Analysis Laboratory and the Max Planck Institute for Plant Breeding Research for providing the sequence-indexed *Arabidopsis* T-DNA insertion mutants; the ABRC and the Nottingham Arabidopsis Stock Centre for providing us with the seeds of *Arabidopsis*; and the NBRP-*E. coli* at the National Institute of Genetics for providing the *E. coli* mutant strains.

References

Alonso JM, Stepanova AN, Leisse TJ, Kim CJ, Chen H, Shinn P, Stevenson DK, Zimmerman J, Barajas P, Cheuk R, et al. (2003) Genome-wide insertional mutagenesis of *Arabidopsis thaliana*. *Science* 301: 653–657

Assaad FF, Signer ER (1990) Cauliflower mosaic virus P35S promoter activity in *Escherichia coli*. *Mol Gen Genet* 223: 517–520

Baba T, Ara T, Hasegawa M, Takai Y, Okumura Y, Baba M, Datsenko KA, Tomita M, Wanner BL, Mori H (2006) Construction of *Escherichia coli* K-12 in-frame, single-gene knockout mutants: The Keio collection. *Mol Syst Biol* 2: 2006 0008 10.1038/msb4100050

Bates PD, Stymne S, Ohlrogge J (2013) Biochemical pathways in seed oil synthesis. *Curr Opin Plant Biol* 16: 358–364

Castanñeda-García A, Rodríguez-Rojas A, Guelfo JR, Blázquez J (2009) The glycerol-3-phosphate permease GlpT is the only fosfomycin transporter in *Pseudomonas aeruginosa*. *J Bacteriol* 191: 6968–6974

Chanda B, Xia Y, Mandal MK, Yu K, Sekine K, Gao Q, Selote D, Hu Y, Stromberg A, Navarre D, et al. (2011) Glycerol-3-phosphate is a critical mobile inducer of systemic immunity in plants. *Nat Genet* 43: 421–427

Clough SJ, Bent AF (1998) Floral dip: A simplified method for *Agrobacterium*-mediated transformation of *Arabidopsis thaliana*. *Plant J* 16: 735–743

Craigon DJ, James N, Okyere J, Higgins J, Jotham J, May S (2004) NASCArrays: a repository for microarray data generated by NASC's transcriptomics service. *Nucleic Acids Res* 32 (Database issue): D575–D577

Eastmond PJ (2004) Glycerol-insensitive *Arabidopsis* mutants: *gli1* seedlings lack glycerol kinase, accumulate glycerol and are more resistant to abiotic stress. *Plant J* 37: 617–625

Elashvili I, Defrank JJ, Culotta VC (1998) *phnE* and *glpT* genes enhance utilization of organophosphates in *Escherichia coli* K-12. *Appl Environ Microbiol* 64: 2601–2608

Emanuelsson O, Nielsen H, von Heijne G (1999) ChloroP, a neural network-based method for predicting chloroplast transit peptides and their cleavage sites. *Protein Sci* 8: 978–984

Fliege R, Flügge UI, Werdan K, Heldt HW (1978) Specific transport of inorganic phosphate, 3-phosphoglycerate and triosephosphates across the inner membrane of the envelope in spinach chloroplasts. *Biochim Biophys Acta* 502: 232–247

Folch J, Lees M, Sloane-Stanley GH (1957) A simple method forthe isolation and purification of total lipids from animal tissues. *J Biol Chem* 226: 497–509

Frohlich KM, Roberts RA, Housley NA, Audia JP (2010) *Rickettsia prowazekii* uses an *sn*-glycerol-3-phosphate dehydrogenase and a novel dihydroxyacetone phosphate transport system to supply triose phosphate for phospholipid biosynthesis. *J Bacteriol* 192: 4281–4288

Gamborg OL, Miller RA, Ojima K (1968) Nutrient requirements of suspension cultures of soybean root cells. *Exp Cell Res* 50: 151–158

Gardiner SE, Roughan PG, Slack R (1982) Manipulating the incorporation of [^{14}C]acetate into different leaf glycerolipids in several plant species. *Plant Physiol* 70: 1316–1320

Gidda SK, Shockey JM, Rothstein SJ, Dyer JM, Mullen RT (2009) *Arabidopsis thaliana* GPAT8 and GPAT9 are localized to the ER and possess distinct ER retrieval signals: Functional divergence of the dilysine ER retrieval motif in plant cells. *Plant Physiol Biochem* 47: 867–879

Goldberg RB, de Paiva G, Yadegari R (1994) Plant embryogenesis: zygote to seed. *Science* 266: 605–614

Gubellini F, Verdon G, Karpowich NK, Luff JD, Boël G, Gauthier N, Handelman SK, Ades SE, Hunt JF (2011) Physiological response to membrane protein overexpression in *E. coli*. *Mol Cell Proteomics* 10: M111.007930

Jefferson RA, Kavanagh TA, Bevan MW (1987) GUS fusions: *β*-glucuronidase as a sensitive and versatile gene fusion marker in higher plants. *EMBO J* 6: 3901–3907

Kitajima A, Asatsuma S, Okada H, Hamada Y, Kaneko K, Nanjo Y, Kawagoe Y, Toyooka K, Matsuoka K, Takeuchi M, et al. (2009) The rice *α*-amylase glycoprotein is targeted from the Golgi apparatus through the secretory pathway to the plastids. *Plant Cell* 21: 2844–2858

Kito M, Pizer LI (1969) Purification and regulatory properties of the biosynthetic L-glycerol 3-phosphate dehydrogenase from *Escherichia coli*. *J Biol Chem* 244: 3316–3323

Kleinboelting N, Huep G, Kloetgen A, Viehoever P, Weisshaar B (2012) GABI-Kat SimpleSearch: New features of the *Arabidopsis thaliana* T-DNA mutant database. *Nucleic Acids Res* 40(Database issue): D1211–D1215

Klöck G, Kreuzberg K (1989) Kinetic properties of a *sn*-glycerol-3-phosphate dehydrogenase purified from the unicellular alga *Chlamydomonas reinhardtii*. *Biochim Biophys Acta* 991: 347–352

Kunst L, Browse J, Somerville C (1988) Altered regulation of lipid biosynthesis in a mutant of *Arabidopsis* deficient in chloroplast glycerol-3-phosphate acyltransferase activity. *Proc Natl Acad Sci USA* 85: 4143–4147

Law CJ, Yang Q, Soudant C, Maloney PC, Wang DN (2007) Kinetic evidence is consistent with the rocker-switch mechanism of membrane transport by GlpT. *Biochemistry* 46: 12190–12197

Lewin A, Mayer M, Chusainow J, Jacob D, Appel B (2005) Viral promoters can initiate expression of toxin genes introduced into *Escherichia coli*. *BMC Biotechnol* 5: 19

Linka M, Jamai A, Weber APM (2008) Functional characterization of the plastidic phosphate translocator gene family from the thermo-acidophilic red alga *Galdieria sulphuraria* reveals specific adaptations of primary carbon partitioning in green plants and red algae. *Plant Physiol* 148: 1487–1496

Lu M, Tang X, Zhou JM (2001) *Arabidopsis NHO1* is required for general resistance against *Pseudomonas* bacteria. *Plant Cell* 13: 437–447

McKee JWA, Hawke JC (1979) The incorporation of [^{14}C] acetate into the constituent fatty acids of monogalactosyldiglyceride by isolated spinach chloroplasts. *Arch Biochem Biophys* 197: 322–332

Murashige T, Skoog F (1962) A revised medium for rapid growth and bioassay with tobacco tissue cultures. *Physiol Plant* 15: 473–497

Ohlrogge J, Browse J (1995) Lipid biosynthesis. *Plant Cell* 7: 957–970

Petsalaki EI, Bagos PG, Litou ZI, Hamodrakas SJ (2006) PredSL: A tool for the N-terminal sequence-based prediction of protein subcellular localization. *Genomics Proteomics Bioinformatics* 4: 48–55

Quettier AL, Shaw E, Eastmond PJ (2008) *SUGAR-DEPENDENT6* encodes a mitochondrial flavin adenine dinucleotide-dependent glycerol-3-P dehydrogenase, which is required for glycerol catabolism and post germinative seedling growth in *Arabidopsis*. *Plant Physiol* 148: 519–528

Ramaiah M, Jain A, Baldwin JC, Karthikeyan AS, Raghothama KG (2011) Characterization of the phosphate starvation-induced glycerol-3-phosphate permease gene family in *Arabidopsis*. *Plant Physiol* 157: 279–291

Roughan PG, Holland R, Slack R (1980) The role of chloroplasts and microsomal fractions in polar-lipid synthesis from [1-14C]acetate by cell-free preparations from spinach (Spinacia oleracea) leaves. *Biochem J* 188: 17–24

Shen W, Li JQ, Dauk M, Huang Y, Periappuram C, Wei Y, Zou J (2010) Metabolic and transcriptional responses of glycerolipid pathways to a perturbation of glycerol-3-phosphate metabolism in *Arabidopsis*. *J Biol Chem* 285: 22957–22965

Schmid M, Davison TS, Henz SR, Pape UJ, Demar M, Vingron M, Scholkopf B, Weigel D, Lohmann JU (2005) A gene expression map of *Arabidopsis thaliana* development. *Nat Genet* 37: 501–506

Song XM, Forsgren A, Janson H (1998) Glycerol-3-phosphate transport in *Haemophilus influenzae*: Cloning, sequencing, and transcription analysis of the *glpT* gene. *Gene* 215: 381–388

Sparace SA, Mudd JB (1985) Phosphatidyiglycerol synthesis in spinach chloroplasts: Characterization of the newly synthesized molecule. *Plant Physiol* 70: 1260–1264

Tanaka Y, Nakamura S, Kawamukai M, Koizumi N, Nakagawa T (2011) Development of a series of gateway binary vectors possessing a tunicamycin resistance gene as a marker for the transformation of *Arabidopsis thaliana*. *Biosci Biotechnol Biochem* 75: 804–807

Weber APM, Schwacke R, Flügge UI (2005) Solute transporters of the plastid envelope membrane. *Annu Rev Plant Biol* 56: 133–164

Xue L, McCune LM, Kleppinger-Sparace KF, Brown MJ, Pomeroy MK, Sparace SA (1997) Characterization of the glycerolipid composition and biosynthetic capacity of pea root plastids. *Plant Physiol* 113: 549–557

Yu K, Soares JM, Mandal MK, Wang C, Chanda B, Gifford AN, Fowler JS, Navarre D, Kachroo A, Kachroo P (2013) A feedback regulatory loop between G3P and lipid transfer proteins DIR1 and AZI1 mediates azelaic-acid-induced systemic immunity. *Cell Rep* 3: 1266–1278

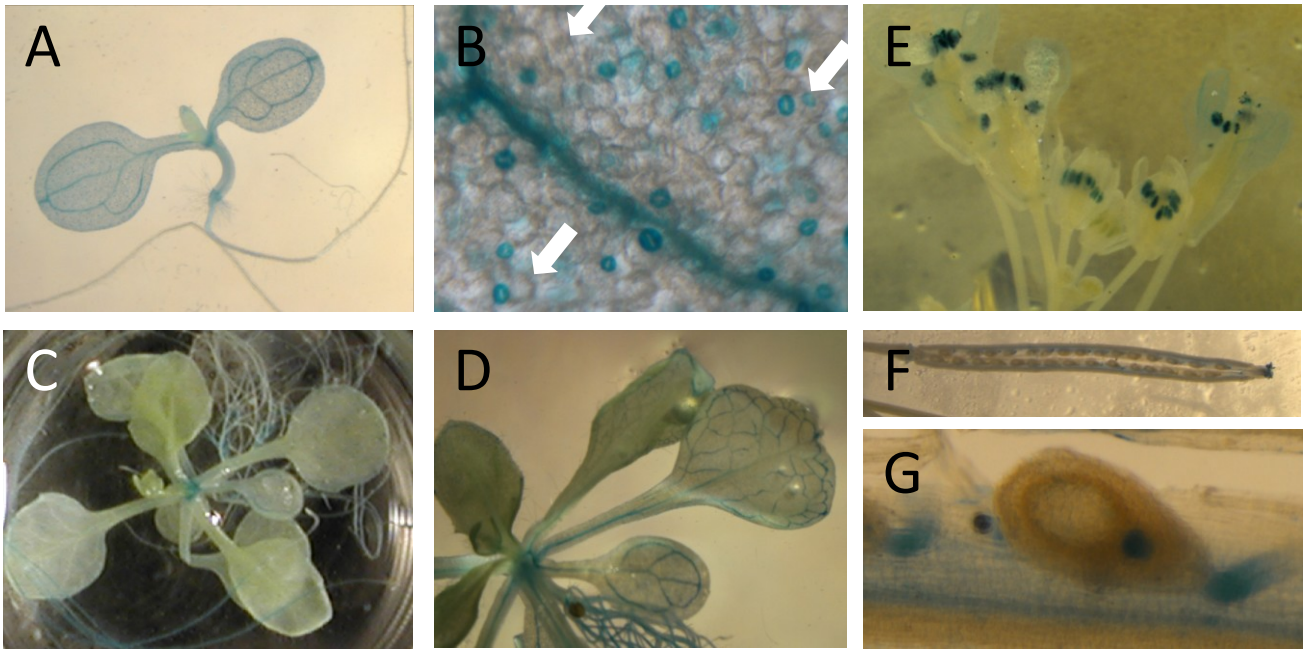

Supplemental Figure S1; Kawai et al., 2014

Supplemental Figure S1. Analysis of *G3Pp4* expression in Arabidopsis seedlings by *Pro*$_{G3Pp4}$*::GUS*. (A) GUS-staining in a 7-d-old seedling grown on agar. (B) GUS-staining is observed in the vascular bundle and the stomata guard cells. (C, D) GUS-staining in a 14-d-old seedling. (E) GUS-staining in flowers is restricted to the stamen. (F) GUS-staining in young silique at 5 d after flowering. (G) GUS-staining in the developing seeds inside silique is observed in the placenta and the embryo.

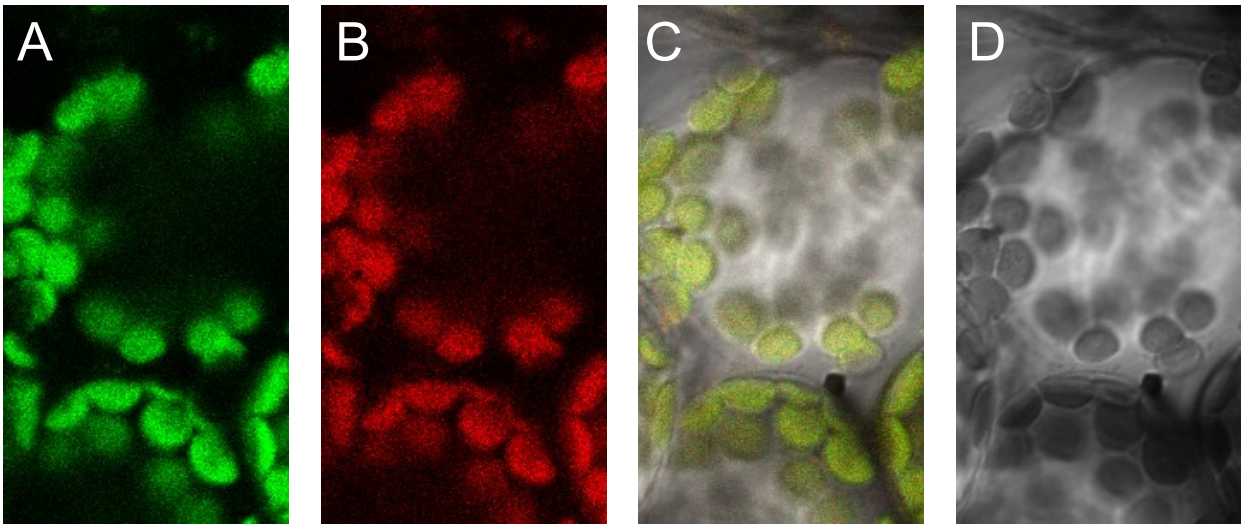

Supplemental Figure S2; Kawai et al., 2014

Supplemental Figure S2. Subcellular localization of EYFP–G3Pp4 in mesophyll cells of transgenic *Arabidopsis* . (A) Fluorescence signal from EYFP–G3Pp4. (B) Autofluorescence of chlorophyll. (C) merged image. (D) DIC image.